Query Details Back to Main Page

1. **Please check if affiliation is presented correctly.**

2. **Please check if the section headings are assigned to appropriate levels.**

3. **Please check if the tables and their values are presented/captured correctly.**

4. **Please check if figure captions are presented/captured correctly.**

Original Article

The examination of stress shielding in a finite element lumbar spine inclusive of the thoracolumbar fascia

Emily Newell, [1]

Emily Newell holds a Bachelor of Engineering from McMaster University, Canada. She is currently pursuing her Ph.D. in Mechanical Engineering at McGill University, Canada, with research focused on the biomechanics of the musculoskeletal system.

Mark Driscoll, [1]✉

Email mark.driscoll@mcgill.ca

Mark Driscoll received his Ph.D. in Biomedical Engineering at École Polytechnique of Montreal. He is currently an Assistant Professor for the Department of Mechanical Engineering at McGill University, Canada. His research focuses on manufacturing and biomechanics.

[1] Musculoskeletal Biomechanics Research Lab, Department of Mechanical Engineering, McGill University, 845 Sherbrooke St. W, Montréal, QC, H3A 0G4 Canada AQ1

Received: 26 November 2020 / Accepted: 4 July 2021

Abstract

Despite the prevalence of low back pain (LBP) in society, the pathomechanism of LBP continues to elude researchers. LBP patients have demonstrated morphological and material property changes to their lumbar soft tissues, potentially leading to irregular load sharing within the lumbar spine. This study aims to analyze potential stress shielding consequential of augmented soft tissue properties via the comparison of a healthy and LBP finite element models. The models developed in this study include the vertebrae, intervertebral discs and soft tissues from L1–S1. Soft tissue morphology and material properties for the LBP model were augmented to reflect documented clinical findings. Model validation preceded testing and was confirmed through comparison to the available literature. Relative to the healthy model, the LBP model demonstrated an increase in stress by 15.6%, with 99.8% of this stress increase being distributed towards the thoracolumbar fascia. The majority of stress skewed towards the fascia may indicate a potential stress allocation bias whereby the lumbar muscles are unable to receive regular loading, leading to stress shielding. This load allocation bias and subsequent stress shielding may potentially contribute to the progression and pathomechanism of LBP but prospective studies would be required to make that link.

Graphical abstract

Development of two musculoskeletal models (one healthy, one with low back pain) for comparative analysis of lumbar soft tissue stress distributions through finite element analysis.

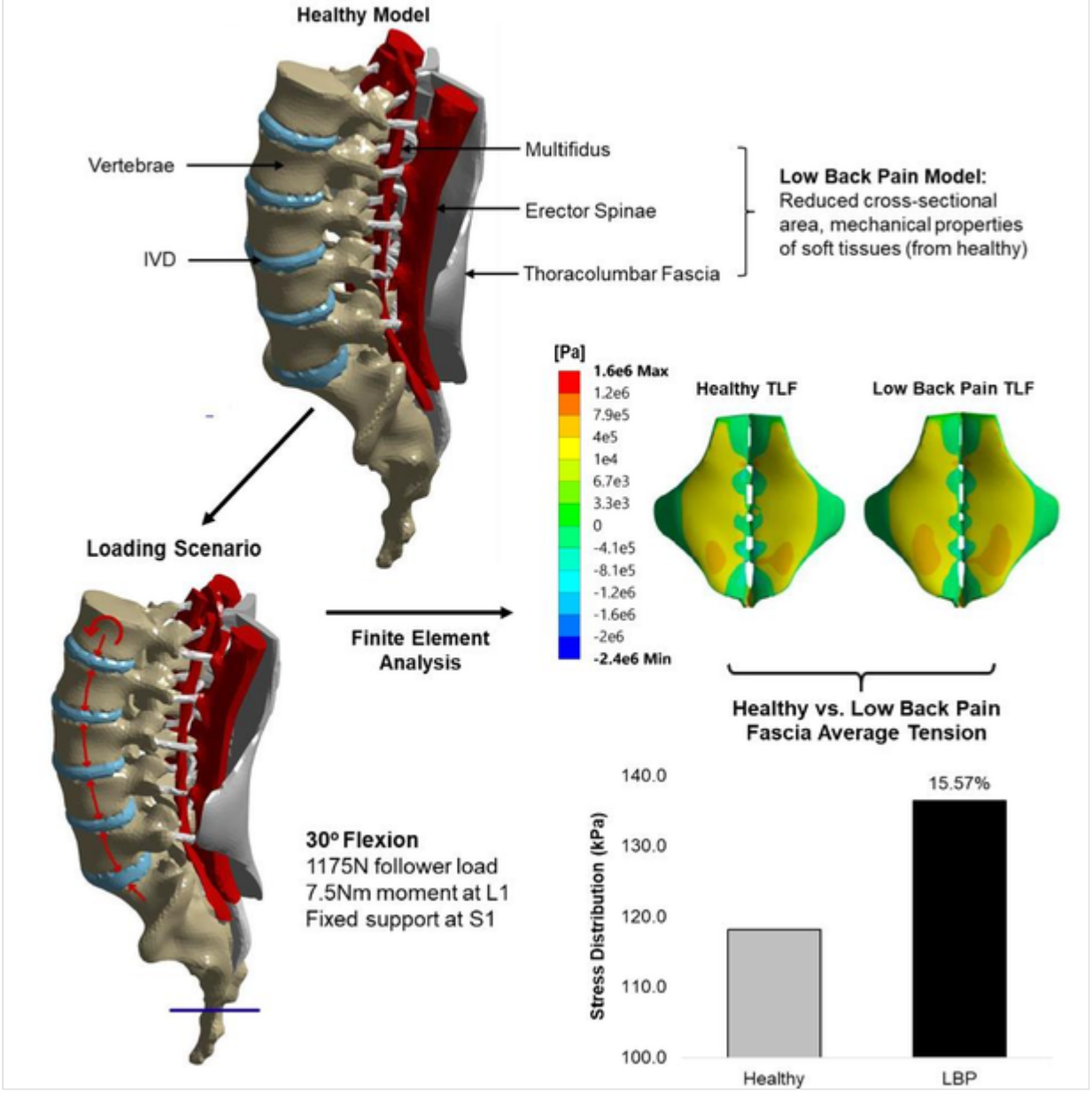

Keywords

Biomechanics
Low back pain
Finite element analysis
Physiological stress shielding
Lumbar fascia

1. Introduction

AQ2

Low back pain (LBP) is a public health crisis. More than 80% of people will experience LBP at least once [1], with upwards of 75% of sufferers enduring a relapse in pain after 12 months of occurrence [2, 3]. While numerous clinical treatments are available to provide pain and disability relief, such as manual therapies and pharmaceuticals, no treatment currently exists to cure LBP, leaving many patients to continue experiencing substantial pain [4]. Moreover, poor treatment efficacy for LBP has resulted in high costs to society, reportedly costing $100–$200 billion annually in the USA alone [5].

Crucially, nearly 85% of all LBP cases cannot be attributed to a specific cause [6], indicating that LBP may not be accurately determined due to the unknown pathophysiological mechanisms that are involved in pain perception in the low back [7]. However, physiological stress shielding may contribute to the development and progression of LBP. Although often attributed to the bone, stress shielding may occur within the soft tissues. Under loading, stronger tissues will withstand the majority of the load, shielding adjacent tissues from experiencing normal loading, leading to poor soft tissue performance.

Soft tissue performance is regulated by tissue remodelling through external trigger mechanisms (e.g. stress), whereby increased stress prompts tissue growth while stimuli-deficient tissues atrophy. Continuous degenerative remodelling may promote irregular force balances, resulting in tissue activation irregularities and cyclical atrophy—a sequence previously suggested in musculoskeletal disorders [8] and demonstrated in scoliotic lumbar tissues [9]. Augmentation of the morphology and mechanical properties of the TLF [10], erector spinae (ES) and multifidus (MF) [11, 12, 13] has been correlated with LBP. These augmentations suggest a potential stress allocation bias within the lumbar spine, potentially laying the foundation for physiological stress shielding. In turn, stress shielding may further distort stress distributions within the lumbar spine, promoting this load allocation bias and leading to cyclical stress shielding. Ultimately, this stress shielding may be detrimental to soft tissues providing spinal stability through a consistent contraction in an effort to avoid degenerative spinal conditions such as LBP [14].

Finite element (FE) modelling, a numerical method which subdivides systems of interest into individual elements, allows for computation of the system's deformation to loading given boundary conditions. Yielding multiple benefits to the medical field, FE allows for non-invasive physiological stress analysis [15] and medical device design [16]. As such, FE provides a useful method for conducting

mechanical analyses of healthy and degenerative spinal conditions. Imperative to the FE process is rigorous validation of the in silico model(s) through comparison to in vitro (i.e. bench testing) or in vivo (i.e. clinical testing) to ensure the models provide a realistic representation of human anatomy and physiology [17].

Thus, the aim of this study is to investigate the potential for stress shielding as a result of altered soft tissue properties found in LBP patients through the comparative analysis of two musculoskeletal finite element models (FEMs)—one healthy and one with LBP.

2. Methods

To investigate the potential for stress shielding within musculoskeletal tissues, two FEMs depicting the lumbar musculoskeletal system were created based on previously validated works [18]: one healthy and one afflicted by LBP. Models were composed of stereolithography (STL) files depicting the vertebrae and intervertebral discs (IVDs) from L1–S1 and associated soft tissues (tendons, the longissimus thoracis (representing the ES and referred to as the ES hereafter), MF and TLF). These STL files were obtained from an anatomography database containing volumetric tissues constructed from a 3D CT-scanned human male and subsequently imported into SpaceClaim (ANSYS V19.1, Canonsburg, Pennsylvania). Soft tissues extending past 10 mm superior to the surface of the L1 vertebra were trimmed and removed.

2.1. Construction of a healthy model

To construct the healthy model, the vertebrae, IVDs, tendons, ES, MF and TLF were modelled as volumetric body bodies. All tissues were assumed to be linear isotropic and near-incompressible. Material properties used for the healthy model were obtained from the literature [13, 19, 20, 21, 22, 23] (Table 1). Tissues were assumed to have a Poisson ratio of 0.45 and the vertebrae were assigned a Poisson's ratio of 0.3 [19]. The model was imported into and assessed with ANSYS Static Structural (ANSYS V19.1, Canonsburg, Pennsylvania).

Table 1

Material properties of anatomical structures used in the healthy and low back pain (LBP) finite element models (FEMs) [12, 13, 19, 20, 21, 22, 23]

AQ3

Tissue	Young's modulus (MPa)	Poisson's ratio (unitless)

Tissue	Young's modulus (MPa)			Poisson's ratio (unitless)		
	Healthy FEM	LBP FEM	% difference	Healthy FEM	LBP FEM	% difference
	Healthy FEM	**LBP FEM**	**% difference**	**Healthy FEM**	**LBP FEM**	**% difference**
Vertebrae	3000	3000	-	0.30	0.30	-
Intervertebral discs	8	8	-	0.45	0.45	-
Tendons	200	200	-	0.45	0.45	-
Multifidus	0.092	0.107	16.7%	0.45	0.45	-
Erector spinae	0.041	0.043	5.7%	0.45	0.45	-
Thoracolumbar fascia	416.67	416.67	-	0.45	0.45	-

2.2. Construction of an LBP model

To construct the LBP model, using the aforementioned healthy model as a baseline, the morphological and material properties were altered to best reproduce the soft tissues of LBP patients. Specifically, the cross-sectional areas (CSAs) of the MF and ES STLs were decreased by an average of 19.0 and 6.9%, respectively, as per clinical data of LBP patients [11]. Likewise, the LBP TLF was increased in CSA by 32.4% to reflect the TLF of LBP patients [10]. Material properties of the MF and ES increased in stiffness by 16.7 and 5.7% respectively to reflect the findings of increased stiffness of the MF and ES within LBP patients relative to healthy subjects [12, 13] (Table 1). The model was then imported into ANSYS Static Structural. Only the previously described changes differ between the two models.

2.3. Loading scenario

To reproduce realistic loading experienced by spinal tissues during physiological motion, 30-degree flexion was selected. This physiological motion was favoured for the MF and ES's contribution to the stability, in terms of engineering equilibrium, of the spine [24]. Both models had identical loading, contacts and boundary conditions. A compressive follower load of 1175 N was applied, with a pure bending moment of 7.5 Nm placed at the centre of the L1 vertebra (Fig. 1) [25]. No loading was placed onto the soft tissues, ensuring passive muscle response. All connections between tissues were bonded. Any contacts between the

TLF, ES and MF were frictionless to prevent frictional stresses. The tail of the S1 was denoted as a fixed support.

Fig. 1

Finite element model of L1-S1 lumbar spine with loading scenario (indicated by red arrows) on the lumbar spine to induce 30-deg flexion. This figure was created using ANSYS Static Structural

AQ4

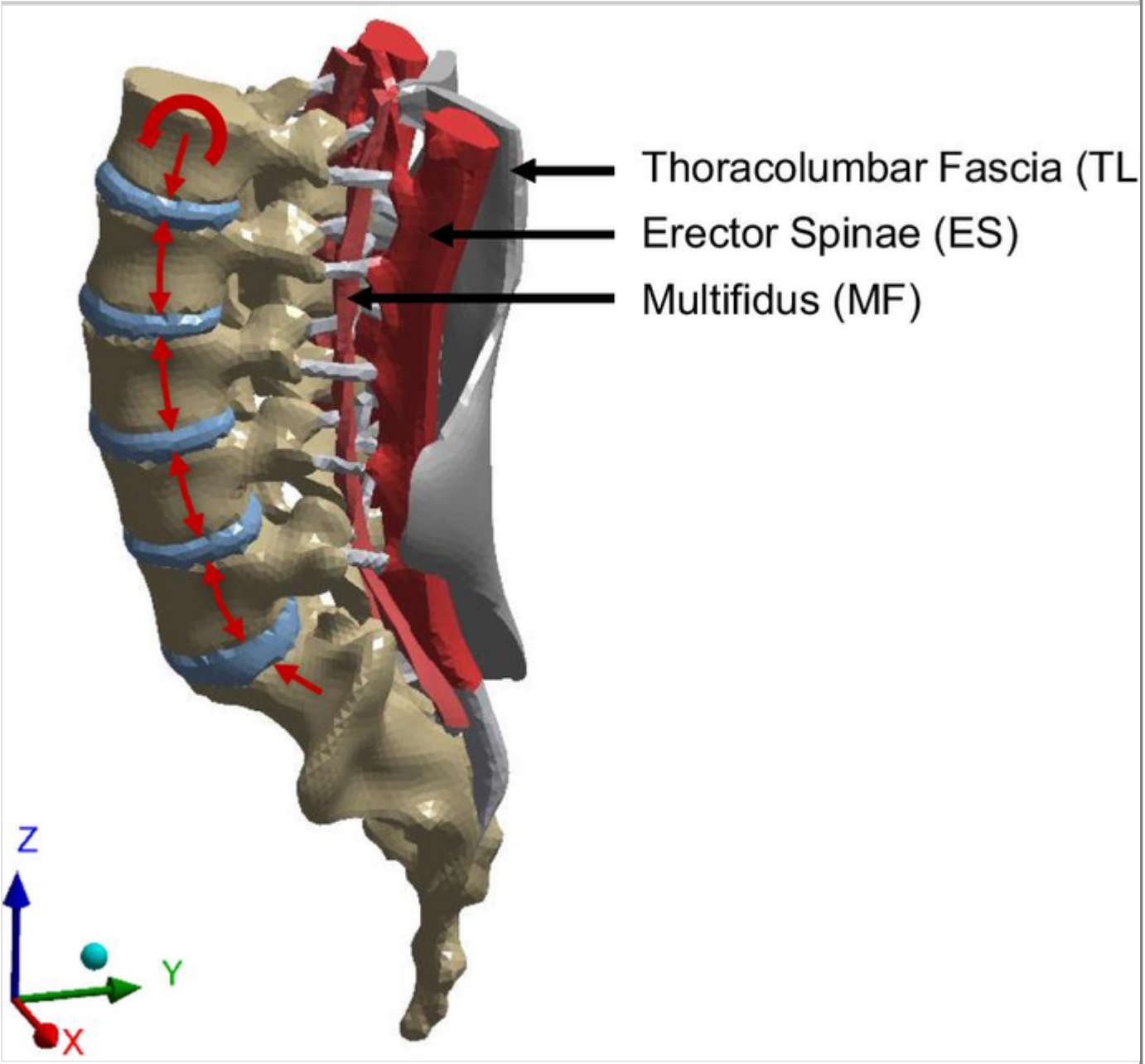

2.4. Evaluation of results and validation

To analyze stress distributions within the soft tissues of the healthy and LBP FEMs, the average tensile stress in the longitudinal direction (+ Z) was calculated (Fig. 1, coordinate system). To do so, the normal stress was obtained for the individual soft tissues in the longitudinal direction (+ Z) at each node through static structural. These results were then exported to MATLAB R2019b (MathWorks, Inc., Natick, Massachusetts). As tissue tension was desired, measured stress at nodes demonstrating compressive stress ($\leq$ 0 Pa) was removed. The resulting stress values at each node were subsequently averaged. The process of calculating the tensile stress was performed for the individual soft tissues (MF, ES and TLF) for both the healthy and LBP FEMs.

For validation purposes, the IVD pressure and intervertebral rotation for both the healthy and LBP FEMs were tabulated for comparison against available literature. The IVD pressure was measured at the centre of each disc in both FEMs to determine the IVD maximum compression. Intervertebral rotation of each vertebra was calculated through the anterior–posterior and superior-inferior translation of a vertebral body point located on the posterior surface relative to a posteroinferior point on the inferior vertebra [26] (Fig. 2). Measurements of these angles were obtained from the model at unflexed and flexed positions (zero-degree and 30-degree flexion, respectively) to determine the change in rotation between vertebral segments. These angles were calculated using MatLab for each vertebral level in both the healthy and LBP FEMs. This methodology was repeated for all vertebral levels in the healthy and LBP FEMs.

Fig. 2

The intervertebral angle of each vertebra is calculated by the difference in angle, θ, between the posterior centroid of a vertebra and the reference point specified in the intermediate inferior vertebra consequential of 30-degree flexion. This figure was created using ANSYS Static Structural and Microsoft Office PowerPoint

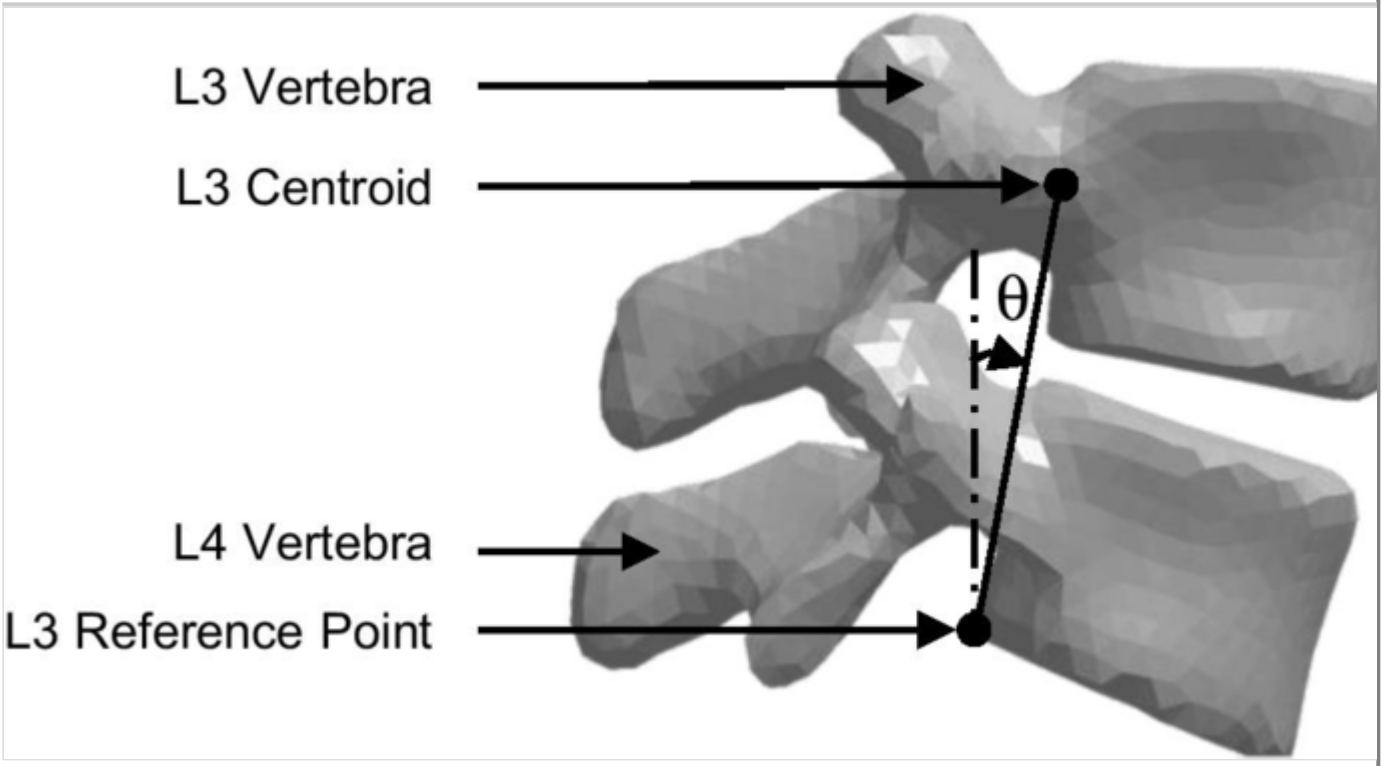

Sensitivity analyses were conducted to evaluate the models' robustness and accuracy. The first test involved using a range of tendon elastic moduli to test model sensitivity to tendon material properties. Another sensitivity analysis involved altering the material properties of the vertebral bodies using elastic modulus values calculated for a composite of cortical and cancellous bone properties. A final test involved varying the mesh size from 3.0 to 1.5 mm.

3. Results

Validation of the healthy and LBP models was obtained through comparison against the median IVD pressure of six clinically validated FEMs [27] through an identical loading scenario to induce 30-degree flexion. Compared to the clinically validated FEMs compiled by Dresicharf et al., the IVD pressures of the healthy and LBP FEMs fall within the "acceptable" range of IVD pressure at the L3/L4 IVD level [27] (Fig. 3). Additionally, the L4/L5 IVD pressure of the healthy and LBP FEM was compared to the L4/L5 IVD pressure measured in vivo during midrange trunk flexion by Wilke et al. [28]. A maximum difference of 0.1 MPa was measured between the L4/L5 IVD pressure of the FEMs and the measured in vivo pressure recorded by Wilke et al. [28]. This validation was further supported by the intervertebral rotation of the FEM vertebral bodies against clinical studies involving patients flexing at 30-degree rotation [29]. All vertebral levels are within

the “validated” range as determined by the clinical study [29] for intervertebral rotation (Fig. 4).

Fig. 3

Healthy and low back pain finite element model (FEM) intervertebral disc (IVD) pressures measured compared to validated literature (“FEM Median” [27], “Wilke et al.” [28]); error bars denote the acceptable range of IVD pressure for FEMs. This figure was created using Microsoft Office Excel and PowerPoint

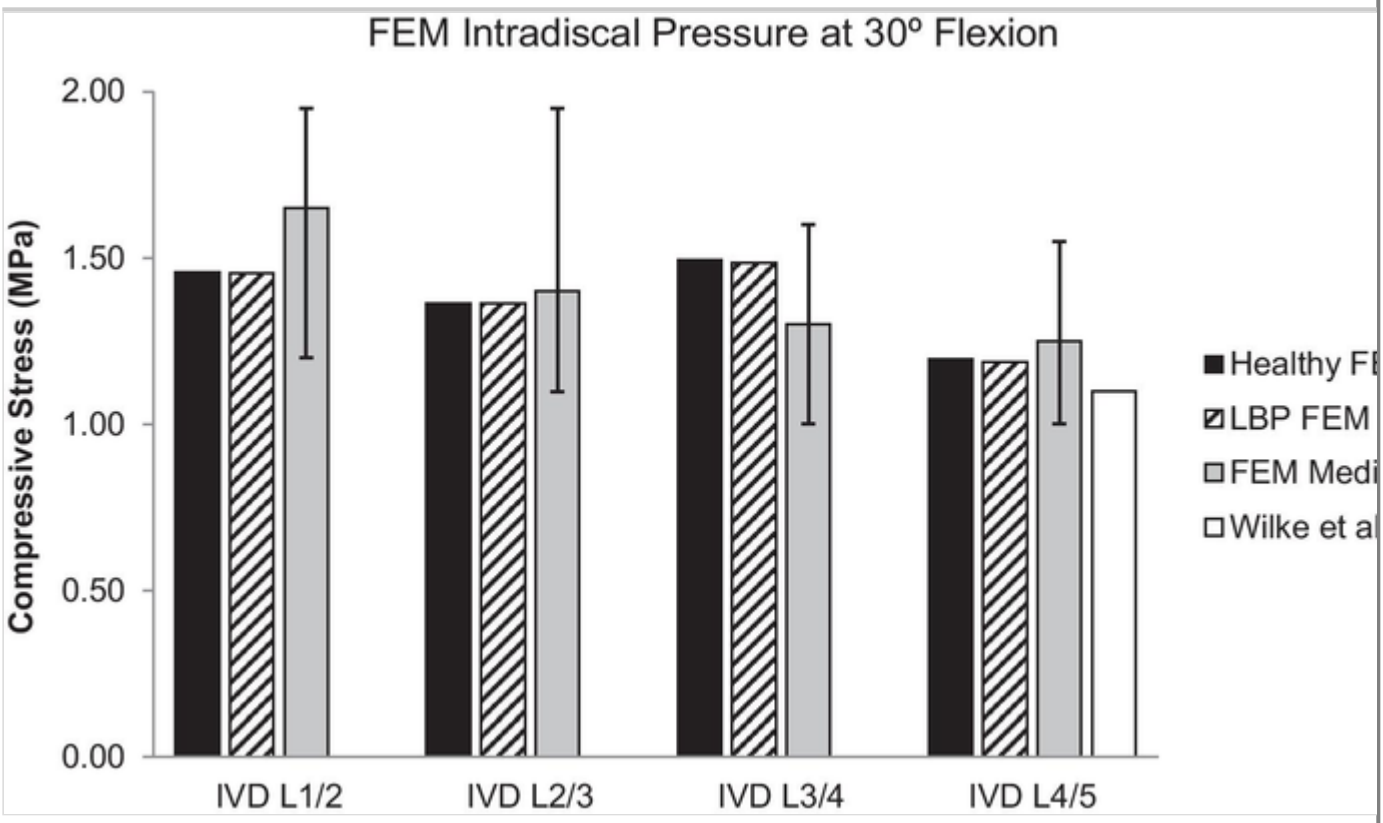

Fig. 4

Healthy and low back pain finite element model intervertebral rotation compared to clinical data [29] in the sagittal plane (trunk flexion). Error bars denote the acceptable range of rotation. This figure was created using Microsoft Office Excel and PowerPoint

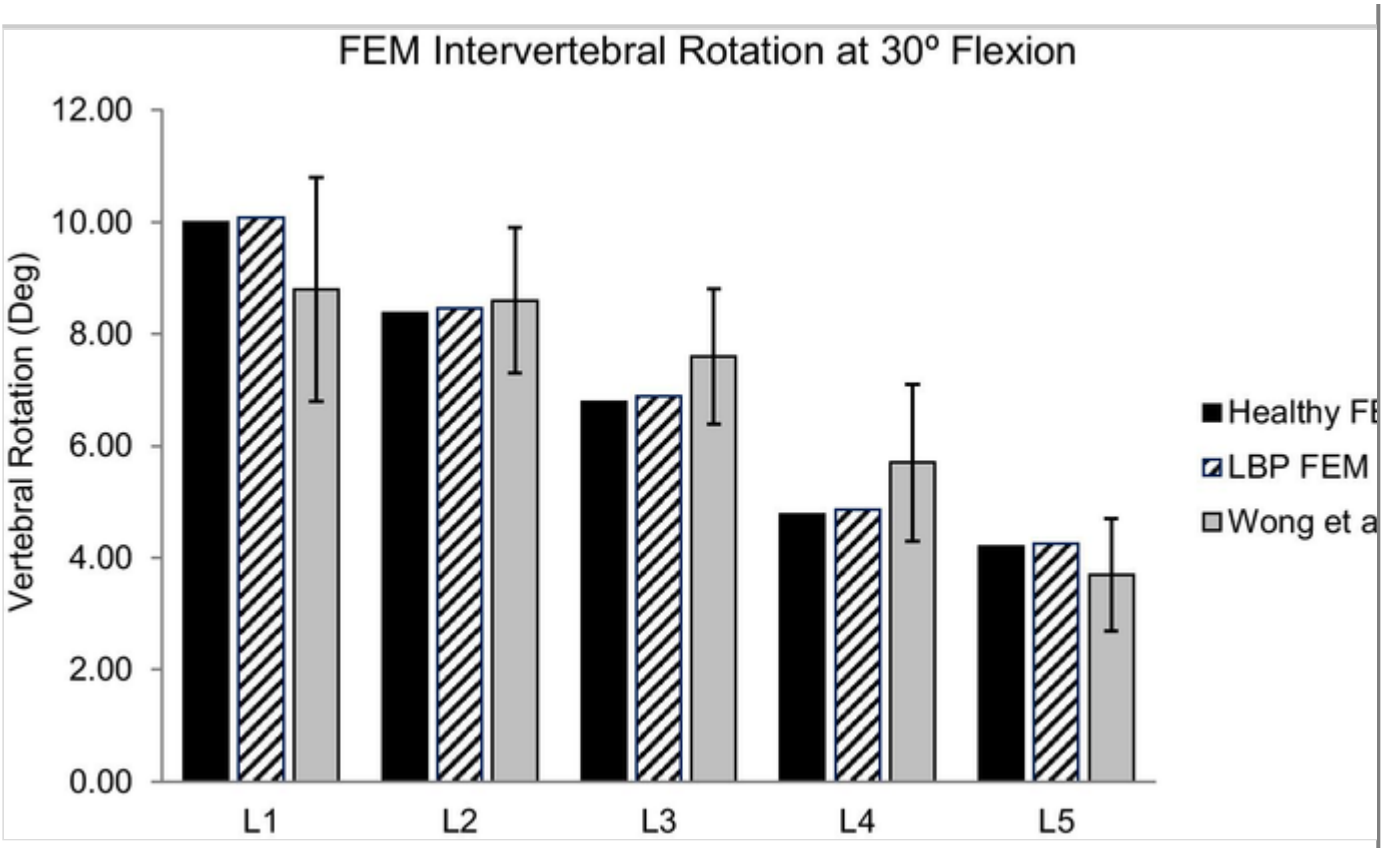

Relative to the healthy FEM, the LBP FEM indicates a decrease in IVD pressure at each IVD level. However, a maximum deviation of 10.0 kPa (a decrease in compression by 0.8%) of IVD pressure occurs at the L4/L5 level. Likewise, there is little difference (< 2%) in intervertebral rotation between FEMs with the largest deviation (an increase of 1.7%) occurring at L4 in the LBP FEM. All results for the IVD pressure and the intervertebral rotation are given in Table 2.

Table 2

Outcome measures of average tension (in kPa), intervertebral disc (IVD) pressure (in MPa) and vertebral rotation (in degrees) for healthy and low back pain (LBP) finite element models (FEMs)

	Healthy FEM	**LBP FEM**	**% Difference**
Avg. tension (kPa)			
Multifidus	0.256	0.289	12.97%
Erector spinae	0.024	0.023	− 4.03%
Thoracolumbar fascia	118.12	136.51	15.57%
Total Avg. tension	118.40	136.82	15.56%
IVD pressure (MPa)			

	Healthy FEM	LBP FEM	% Difference
L1/L2	1.457	1.454	− 0.21%
L2/L3	1.364	1.362	− 0.12%
L3/L4	1.494	1.486	− 0.56%
L4/L5	1.198	1.188	− 0.83%
L5/S1	1.079	1.074	− 0.49%
Vertebral rotation (deg)			
L1	10.00	10.08	0.83%
L2	8.38	8.46	0.97%
L3	6.79	6.89	1.45%
L4	4.78	4.87	1.75%
L5	4.20	4.26	1.38%

The average tensile stress in the MF, ES and TLF for both healthy and LBP FEMs are also reported in Table 2. Despite both FEMs undergoing an identical loading scenario, the average tensile stress experienced by all soft tissues of the LBP FEM increased by a total of 18.4 kPa (15.6%) relative to the healthy FEM. The LBP TLF demonstrated an 18.4 kPa (15.6%) increase in average tensile stress relative to the healthy FEM's TLF. The LBP MF demonstrated an increase in average tensile stress of 33.2 Pa (13.0%), while the LBP ES demonstrated a decrease in average tension by 1.0 Pa (− 4.0%), respectively, relative to the healthy FEM.

Sensitivity analyses further assessed the above findings to explore assumptions used in the development of the FEMs. Variation of the elastic modulus of the tendon yielded a < 5% difference in results from the initially chosen tendon properties, supporting the robustness of the model to tendon modulus. The sensitivity analysis conducted for vertebral material properties demonstrated a change of < 1% when using material properties based on the vertebrae as a composite of cancellous and cortical components. Finally, the mesh sensitivity test generated a maximum deviation in results of < 11%.

4. Discussion

While utilizing FEM has provided a means for analyzing complex physiology, few FEMs provide insight into debilitating musculoskeletal conditions. As such, to the

authors' knowledge, the FEM depicted in this study is the first to portray a lumbar spine having initial conditions reflective of LBP. Additionally, previous FEMs of healthy spines often opted to exclude muscle tissue [25, 27]. Such an assumption ignores the muscles' passive contributions to engineering spinal stability and biomechanical behaviour. Recent in silico studies have favoured follower loads to address the active role of the muscles in spinal biomechanics, but such studies often neglect the passive component of muscle activity. Moreover, the omission of soft tissues within FEMs neglects the role these tissues play in passive force transmission. The fascia has recently been documented to demonstrate a passive role in force transmission [30], potentially providing new insights when included in musculoskeletal FEMs. As such, the inclusion of a follower load within the loading scenario to induce flexion may indirectly capture the active portion of the muscles to stabilize the spine during physiological motion. With the inclusion of volumetric geometry representing the soft tissues, specifically the lumbar muscles and TLF, the passive components of these tissues towards tension production during physiological motion have also been included within the FEM. As such, the models presented here can be considered to capture both active and passive contributions of the soft tissues during physiological motion. In this respect, both FEMs developed in this study provide novelty for the inclusion of soft tissues, specifically the TLF, to account for the passive contribution of the soft tissues.

Inducing 30-degree flexion within the FEMs allowed for an objective comparison of the effects of LBP in relation to that of a healthy spine. While much inter-subject variability exists between spinal profiles with and without LBP, the use of a healthy spinal profile augmented to reflect soft tissue alterations correlated with LBP provides an objective means to investigate the direct effects of augmented soft tissue properties on the spine's biomechanics. Moreover, flexion provides a comparative insight into stress distributions of soft tissues whose primary functions involve spinal stability during flexion, in both healthy and LBP conditions.

Results obtained demonstrated a discrepancy within the IVD pressure, with LBP IVDs yielding an overall decrease in pressure relative to healthy IVDs, and a maximum deviance occurring in the L4/L5 IVD. A decrease in IVD pressure may suggest a reduced ability for the spine to withstand regular loading, with potential consequences on activation patterns for spine-stabilizing muscles. These results, however, will require further investigation. A second discrepancy revealed a total increase in average tensile stress by 18.4 kPa (15.6%) in the LBP soft tissues relative to the healthy soft tissues. However, the MF and ES only withstand 0.2% of this 18.4-kPa stress increase. The remaining 99.8%, however, is distributed towards

the TLF. Furthermore, the ES demonstrated a decrease in average tension by − 4.0% while the MF increased by 13.0%, indicating that the MF withstands the majority of the 0.2% increase in overall average tension exhibited by the LBP FEM paraspinals. Despite the MF and ES being major contributors to spinal stability during flexion, this skewed stress distribution towards the TLF indicates a heavy reliance on the fascia for spines with LBP.

A load allocation bias within lumbar soft tissues may exist as indicated by the increased average tensile stress being skewed towards the TLF. This load allocation bias may instigate stress shielding whereby the TLF effectively shields the MF and ES from loading. Reduced loading on the MF and ES may result in tissue atrophy through physiological remodelling, preventing the tissues from withstanding normal loading during motion. Given the MF and ES's contribution to the stability of the spine, reduced loading capacity may have dire consequences on spinal stability. To compensate for this, irregular muscle activation of other soft tissues may be recruited—a scenario demonstrated in LBP patients with compromised paraspinal morphology [31]. These newly activated tissues undergo elevated loading, resulting in positive physiological remodelling. The increase in TLF CSA for LBP patients [10] provides further support of elevated stresses triggering positive tissue remodelling. Tissue growth may result in the TLF withstanding higher loading, further shielding the MF and ES, effectively trapping the lumbar soft tissues in cyclical physiological remodelling due to the load allocation bias (Fig. 5). Long-term, cyclical stress shielding may result in further deterioration of the lumbar soft tissues, potentially leading to further progression of LBP. Additionally, the onset of changes to lumbar soft tissues' mechanical properties, eventually leading to a load allocation bias and stress shielding, may be a contributing factor to the onset of LBP. Such a sequence of cyclical stress shielding has also been hypothesized to occur within musculoskeletal systems depicting unilateral LBP [32]. Future studies will be required to further investigate stress shielding's role in the pathomechanism of LBP.

Fig. 5

Degenerative cycle of remodelling within low back pain. This figure was created using Microsoft Office PowerPoint

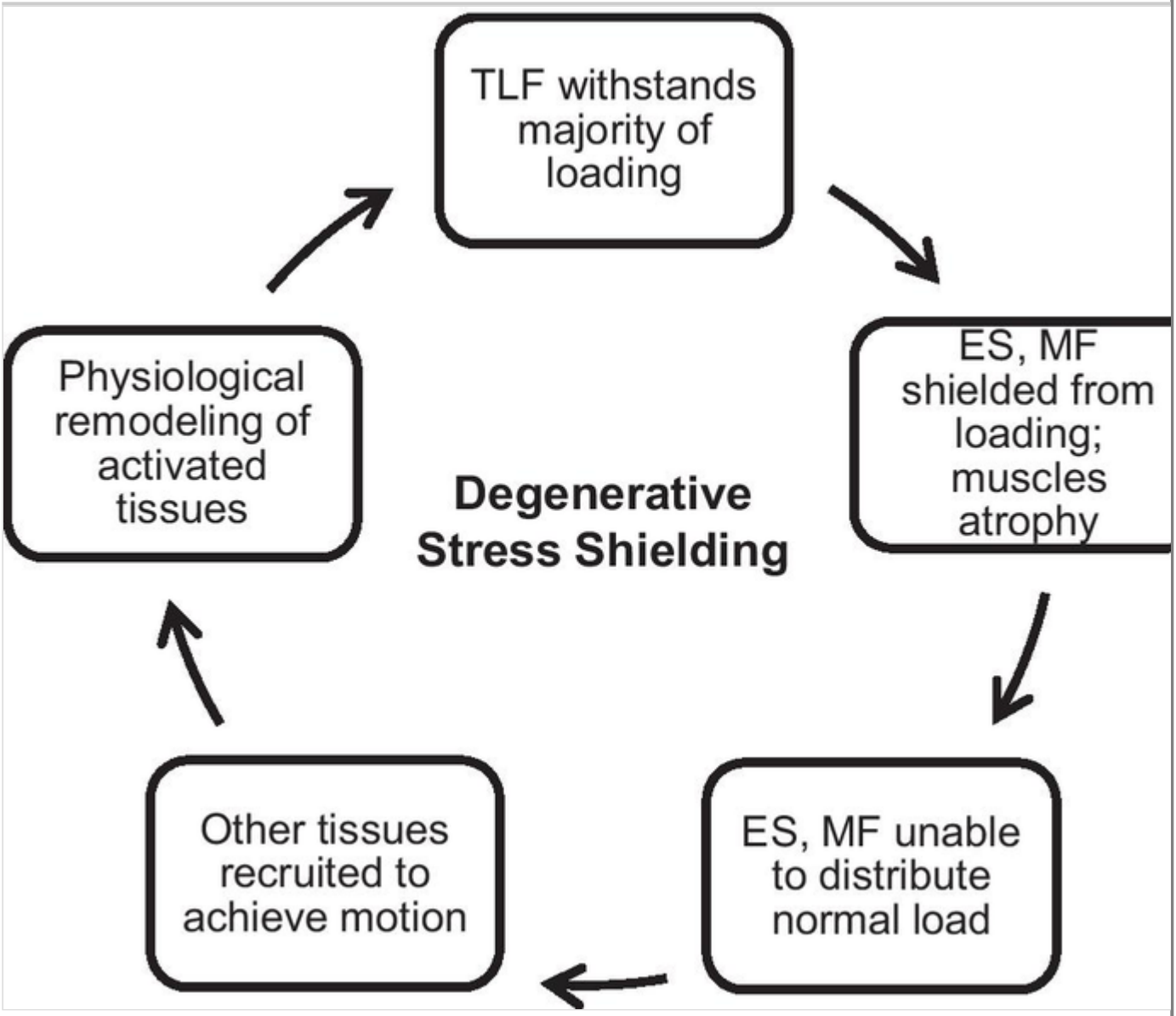

Both FEMs created in this study were indirectly validated through comparison with published literature. The healthy and LBP FEMs demonstrated good agreement with respect to IVD pressure compared to multiple, validated in silico models and a clinical study measuring the L4/L5 IVD pressure in vivo. These validated FEMs each used patient-specific geometry and varying material properties. The median of the IVD pressure obtained from these FEMs, as well as the maximum and minimum IVD pressures, were measured, providing a range of “validated” IVD pressure values which agree with in vivo and in vitro IVD pressures [27]. The healthy and LBP FEMs’ IVD pressures were within the max–min “validated range” of values for each lumbar IVD obtained from the compiled in silico models, indicating the developed FEMs may be considered indirectly validated. Additionally, the minor difference between the L4/L5 IVD pressure obtained from the healthy and LBP FEMs, and the L4/L5 pressure measured in vivo provides further support for the

validation of the models. Likewise, results obtained for intervertebral rotation of the healthy and LBP FEMs were within the obtained range (average ± std. dev) of results for rotation of each vertebral body provided by the clinical study, reaffirming the models' validity to execute the experimental condition explored herein. In addition to the aforementioned validity achieved for the FEMs, future studies should involve the development of a clinical classification or regression analysis regarding the effects of physiological stress shielding with respect to the pain experienced by LBP sufferers. Such a classification/analysis would require a long-term study composed of multiple clinical trials involving nonspecific LBP suffers but would allow for further support of the discussions put forth regarding the validation above and would be the highest applicable experimental model.

To develop realistic spine models demonstrating LBP, assumptions were required. First, the FEMs' geometry was obtained from an anatomagraphic database developed from MRIs of a young, healthy adult male [33]. With in vivo studies, there may be inter-subject variability in tissue geometry, which may cause difficulty in determining objective consequences on spinal biomechanics as a result of LBP. As the constructed FEMs use identical STL files to represent spinal tissues, inter-subject variability does not factor into the results obtained. As this study constructed two FEMs using STL files of the same tissue, inter-subject variability within the study was avoided.

Additional assumptions included the simplification of the tissues included within the FEMs. Although vertebrae are composites of cortical and cancellous bone, the FEM vertebral material properties were homogenous. However, sensitivity analysis testing demonstrated vertebral body material properties demonstrated little effect on the models' results. Moreover, all FEM material properties were modelled as homogenous linear isotropic, yet biological tissues are inhomogeneous, viscoelastic and anisotropic in nature. Soft tissue material properties were selected from previously validated in silico studies and other clinical studies. Tendon material properties were unavailable from previous clinical studies. However, a sensitivity analysis concluded tendon material properties do not affect the models' results.

The FEMs demonstrated good agreement with respect to IVD pressure when compared to multiple osteoligamentous in silico models with varying material properties, including non-linear, anisotropic and hyper-elastic properties for anatomical tissues when undergoing an identical loading scenario for midrange flexion. To further support this validation, a comparison of L4/L5 IVD pressure showed little deviation when compared to clinical studies measuring IVD pressure

during midrange trunk flexion. Thus, the use of linear elastic properties for the anatomical tissues included within the healthy and LBP FEMs may be considered acceptable. Additionally, the models outlined within this study were analyzed statically. As such, the time-dependent, viscoelastic properties of the tissues were negated due to the exclusion of time. Should future studies investigate the dynamic change in stress distributions between healthy and LBP soft tissues, it is imperative to include the time-dependent material behaviours of these tissues.

Furthermore, the FEMs developed for this study excluded tissues deemed unnecessary for the analysis of the average tissue tension developed within the lumbar muscles and TLF (e.g. ligaments, vertebral endplates). However, the comparison to the aforementioned osteoligamentous in silico models undergoing an identical loading scenario demonstrated good agreement in lumbar IVD pressure despite the exclusion of these tissues within the FEMs. Likewise, the comparison to the clinical studies for intervertebral rotation and IVD pressure within human subjects also demonstrated good agreement. Thus, the validation methods suggest the healthy and LBP FEMs provide a realistic representation of musculoskeletal biomechanics under physiological motion and within the content in which the present study derived its relative results. Lastly, the use of simplified anatomy and material properties reduced the overall computational and time requirements of the FEMs, allowing for optimization of the models without sacrificing the accuracy of the obtained results. Mesh sensitivity testing indicated the models were unaffected by mesh sizing. Therefore, through multiple sensitivity analyses, the models may be considered robust.

This study sought to analyze the effects of changes to the morphological and mechanical properties of soft tissues associated with LBP as a means to investigate the potential for physiological stress shielding to contribute to the onset or progression of LBP. However, physiological stress shielding may not be isolated to nonspecific LBP conditions. Future investigations into physiological stress shielding within LBP musculoskeletal systems should include conditions associated with LBP (e.g. disc degeneration, spondylolisthesis) in addition to changes in morphological and material property changes of the muscles. Such studies will provide further insight into stress shielding’s potential role in the progression of LBP, regardless if idiopathic.

5. Conclusion

This novel study aimed to analyze the potential for stress shielding within the musculoskeletal soft tissues through the comparative analysis of a healthy and LBP

lumbar spine. Results demonstrated an overall increase in average tension in the musculoskeletal system afflicted by LBP, with the majority of stress skewed towards the TLF. The absence of this load allocation bias within the healthy FEM may indicate the occurrence of physiological stress shielding in LBP patients.

Publisher's note

Author contributions

All authors contributed to the study conception and design. Methodology, data collection and analysis and validation were performed by Emily Newell. The first draft of the manuscript was written by Emily Newell. Review and editing were performed by all authors on previous versions of the manuscript. All authors read and approved the final manuscript.

Funding

This study was funded by the Fonds de Recherche du Québec – Nature et Technologies (FRQNT, grant no. NC-205220) and the Natural Science and Engineering Research Council (NSERC, grant no. NSERC GP514085-17).

Declarations

Conflict of interest The authors declare no competing interests.

References

1. Andersson GBJ (1999) Epidemiological features of chronic low-back pain. The Lancet 354:581–585

2. Hestbaek L, Leboeuf-Yde C, Manniche C (2003) Low back pain: what is the long-term course? A review of studies of general patient populations. Eur Spine J 12:149–165. https://doi.org/10.1007/s00586-002-0508-5

3. Croft PR, Macfarlane GJ, Papageorgiou AC et al (1998) Outcome of low back pain in general practice. Br Med J 316:1356–1359. https://doi.org/10.1136/bmj.317.7165.1083

4. Maher C, Underwood M, Buchbinder R (2017) Non-specific low back pain. The Lancet 389:736–747

5. Katz JN (2006) Lumbar disc disorders and low-back pain: socioeconomic factors and consequences. J Bone Jt Surg 88:21–24. https://doi.org/10.2106/JBJS.E.01273

6. Deyo RA, Weinstein JN (2001) Low back pain. N Engl J Med 344:363–370. https://doi.org/10.1136/bmj.322.7293.1027

7. Borenstein D, Calin A (2012) Causes of low back pain. In: Fast facts: low back pain, 2nd ed. Heath Press Ltd., Abingdon, UK, pp 46–72

8. Driscoll M, Blyum L (2011) The presence of physiological stress shielding in the degenerative cycle of musculoskeletal disorders. J Bodyw Mov Ther 15:335–342. https://doi.org/10.1016/j.jbmt.2010.05.002

9. Driscoll M, Aubin CE, Moreau A et al (2009) The role of spinal concave-convex biases in the progression of idiopathic scoliosis. Eur Spine J 18:180–187. https://doi.org/10.1007/s00586-008-0862-z

10. Langevin HM, Konofagou EE, Badger GJ et al (2011) Reduced thoracolumbar fascia shear strain in human chronic low back pain. BMC Musculoskelet Disord 12:1–11. https://doi.org/10.1186/1471-2474-12-203

11. Kamaz M, Kireşi D, Oğuz H et al (2007) CT measurement of trunk muscle areas in patients with chronic low back pain. Diagn Interv Radiol 13:144–148

12. Masaki M, Aoyama T, Murakami T et al (2017) Association of low back pain with muscle stiffness and muscle mass of the lumbar back muscles, and sagittal spinal alignment in young and middle-aged medical workers. Clin Biomech 49:128–133. https://doi.org/10.1016/j.clinbiomech.2017.09.008

13. Masaki M, Ji X, Yamauchi T et al (2019) Effects of the trunk position on muscle stiffness that reflects elongation of the lumbar erector spinae and multifidus muscles: an ultrasonic shear wave elastography study. Eur J Appl Physiol 119:1085–1091. https://doi.org/10.1007/s00421-019-04098-6

14. Cholewicki J, McGill SM (1996) Mechanical stability of the in vivo lumbar spine: implications for injury and chronic low back pain. Clin Biomech 11:1–15. https://doi.org/10.1016/0268-0033(95)00035-6

15. Rayfield EJ (2007) Finite element analysis and understanding the biomechanics and evolution of living and fossil organisms. Annu Rev Earth Planet Sci 35:541–576. https://doi.org/10.1192/bjp.112.483.211-a

16. Driscoll M (2019) The impact of the finite element method on medical device design. J Med Biol Eng 39:171–172. https://doi.org/10.1192/bjp.112.483.211-a

17. American Society of Mechanical Engineers (2018) Assessing credibility of computational modeling through verification and validation: application to medical devices. American Society of Mechanical Engineers, New York, NY, USA

18. El Bojairami I, El Monajjed K, Driscoll M (2020) Development and validation of a timely and representative finite element human spine model for biomechanical simulations. Sci Rep 10:1–16. https://doi.org/10.1038/s41598-020-77469-1

19. Smit T, Odgaard A, Schneider E (1999) Structure and function of vertebral trabecular bone. Spine 22:2823–2833

20. Yang H, Nawathe S, Fields AJ, Keaveny TM (2012) Micromechanics of the human vertebral body for forward flexion. J Biomech 45:2142–2148. https://doi.org/10.1016/j.jbiomech.2012.05.044

21. Bonilla KA, Pardes AM, Freedman BR, Soslowsky LJ (2018) Supraspinatus tendons have different mechanical properties across sex. J Biomech Eng 141:011002. https://doi.org/10.1115/1.4041321

22. Yahia LH, Pigeon P, DesRosiers EA (1993) Viscoelastic properties of the human lumbodorsal fascia. J Biomed Eng 15:425–429. https://doi.org/10.1016/0141-5425(93)90081-9

23. Creze M, Soubeyrand M, Yue JL et al (2018) Magnetic resonance elastography of the lumbar back muscles: a preliminary study. Clin Anat

31:514–520. https://doi.org/10.1002/ca.23065

24. Marieb EN, Hoehn K (2013) The muscular system. In: Beauparlant S, Puttkamer G, Cutt S, et al (eds) Human anatomy & physiology, 9th ed. Pearson, Boston, USA, pp 319–386

25. Rohlmann A, Zander T, Rao M, Bergmann G (2009) Realistic loading conditions for upper body bending. J Biomech 42:884–890. https://doi.org/10.1016/j.jbiomech.2009.01.017

26. Lin RM, Yu CY, Chang ZJ, Su FC (1994) Flexion-extension rhythm in the lumbosacral spine. Spine 19:2204–2209. https://doi.org/10.1097/00007632-199410000-00015

27. Dreischarf M, Zander T, Shirazi-Adl A et al (2014) Comparison of eight published static finite element models of the intact lumbar spine: predictive power of models improves when combined together. J Biomech 47:1757–1766. https://doi.org/10.1016/j.jbiomech.2014.04.002

28. Wilke H, Neef P, Caimi M et al (1999) New in vivo measurements of pressures in the intervertebral disc in daily life. Spine 24:755–762

29. Wong KWN, Leong JCY, Chan MK et al (2004) The flexion-extension profile of lumbar spine in 100 healthy volunteers. Spine 29:1636–1641. https://doi.org/10.1097/01.BRS.0000132320.39297.6C

30. Schleip R, Naylor IL, Ursu D et al (2006) Passive muscle stiffness may be influenced by active contractility of intramuscular connective tissue. Med Hypotheses 66:66–71. https://doi.org/10.1016/j.mehy.2005.08.025

31. Danneels LA, Vanderstraeten GG, Cambier DC et al (2000) CT imaging of trunk muscles in chronic low back pain patients and healthy control subjects. Eur Spine J 9:266–272

32. Newell E, Driscoll M (2021) Investigation of physiological stress shielding within lumbar spinal tissue as a contributor to unilateral low back pain: a finite element study. Comput Biol Med 133:1–8. https://doi.org/10.1016/j.compbiomed.2021.104351

33. Okubo K, Tamura T, Takagi T et al (2008) BodyParts3D: 3D structure database for anatomical concepts. Nucleic Acids Res 37:D782–D785. https://doi.org/10.1093/nar/gkn613